Phonons in the ordered $c(2 \times 2)$ phases of Na and Li on Al(001)

2007 J. Phys.: Condens. Matter 19 266005

(http://iopscience.iop.org/0953-8984/19/26/266005)

IOP PUBLISHING JOURNAL OF PHYSICS: CONDENSED MATTER

J. Phys.: Condens. Matter **19** (2007) 266005 (12pp) doi:10.1088/0953-8984/19/26/266005

Phonons in the ordered $c(2 \times 2)$ phases of Na and Li on Al(001)

G G Rusina[1], S V Eremeev[1], S D Borisova[1], I Yu Sklyadneva[1,2], P M Echenique[2,3] and E V Chulkov[2,3]

[1] Institute of Strength Physics and Materials Science SB RAS, 634021, Tomsk, Russia
[2] Donostia International Physics Center (DIPC), 20018 San Sebastián/Donostia, Basque Country, Spain
[3] Departamento de Física de Materiales and Centro Mixto CSIC-UPV/EHU, Facultad de Ciencias Químicas, UPV/EHU, Apartado 1072, 20080 San Sebastián/Donostia, Basque Country, Spain

E-mail: rusina@ispms.tsc.ru

Received 23 February 2007, in final form 25 February 2007
Published 4 June 2007
Online at stacks.iop.org/JPhysCM/19/266005

Abstract

The vibrational properties of the Al(001)-$c(2 \times 2)$–Na (Li) ordered phases formed by alkali atoms (Na and Li) on the Al(001) surface at low and room temperatures are presented. The equilibrium structural characteristics, phonon dispersions and polarization of vibrational modes as well as the local density of phonon states are calculated using the embedded-atom method. The obtained structural parameters are in close agreement with experimental data.

1. Introduction

Alkali-metal (AM) adsorption on metal surfaces has been of considerable interest, partly because it causes a drastic change of many substrate properties [1, 2]. In particular, the formation of submonolayer structures influences the substrate surface electronic states and also gives rise to new adsorbate-induced electron states as well as vibrational modes related to adatoms [3–10]. Many experimental and theoretical studies have been devoted to the structural and electronic properties of aluminium surfaces upon the AM adsorption [4, 5, 9–15]. The main common feature of these adsorption systems is that they have different structures at low and room temperatures because at room temperature the adsorption process involves a temperature-activated vacancy formation on the surfaces, and the adsorbate atoms occupy these vacancies to form ordered substitutional structures [2]. Thus, adsorption of $\frac{1}{3}$ of a monolayer (ML) of Na (Li) at room temperature on the Al(111) surface leads to the formation of the Al(111)-$(\sqrt{3} \times \sqrt{3})$R30°–Na (Li) phase in which the alkali atoms are adsorbed in substitutional sites while at low temperature the Na atoms occupy hollow sites [13–15]. The data obtained for adsorption of $\frac{1}{2}$ ML Na on the Al(001) surface are similar. At room temperature the ordered substitutional $c(2 \times 2)$ structure is formed [14, 16–21]. However, the substitution is not perfect and the Na adlayer lies above the substrate due to the mismatch of the atomic radii. Adsorption

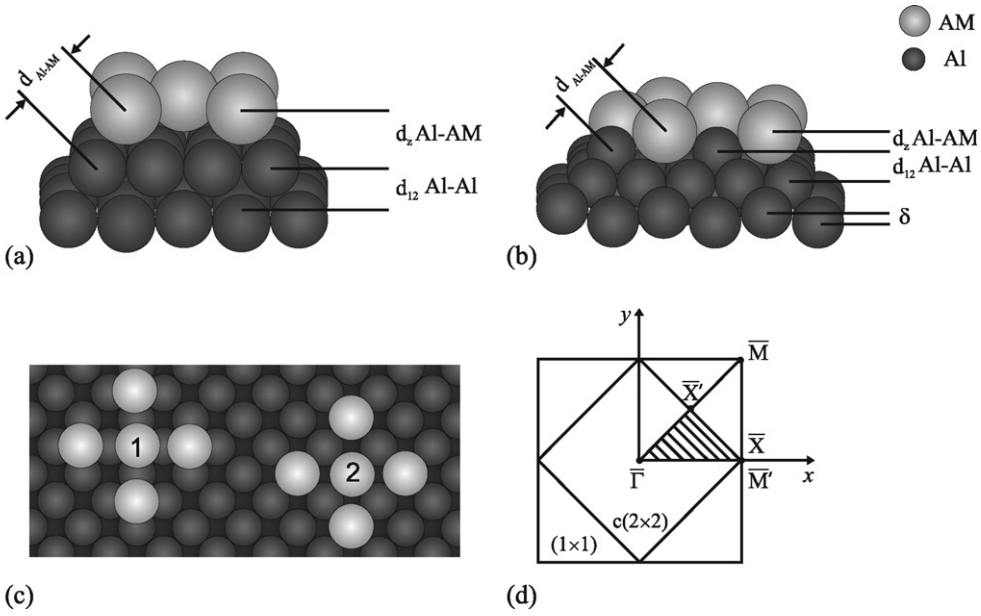

Figure 1. Atomic structure of the Al(001)-$c(2 \times 2)$–alkali metal (Na, Li) adsorbed system: side view for (a) hollow adsorption sites and (b) substitutional adsorption sites (the larger and light circles represent alkali metal atoms and darker circles indicate Al atoms); (c) top view for hollow (1) and substitutional (2) structures; and (d) surface Brillouin zone for the (1×1) and $c(2 \times 2)$ surface structures (the irreducible part of the BZ for $c(2 \times 2)$ is hatched).

of Li on Al(001) at low temperature does not lead to the formation of an ordered structure, and as is shown in low-energy electron diffraction (LEED) experiments some Al atoms are substituted by Li even at 120 K [22]. The ordered Al(001)-$c(2 \times 2)$–Li phase formed by Li adatoms at room temperature is a substitutional surface alloy [21–23] whose structure is similar to that reported for the Al(001)-$c(2 \times 2)$–Na phase.

Detailed experimental investigations of the vibrational properties for alkali-metal adsorbates on Al(111) have been carried out [5, 9]. The results obtained were then interpreted in terms of a semiempirical lattice dynamical model based on the first-neighbour force constant fitted to the bulk empirical data. The vibrational modes of the adsorbate-induced superstructures have also been studied using interaction potentials from the embedded-atom method [10]. No data are available for the Al(001)-$c(2\times2)$–Na (Li) adsorption structures which can be expected to exhibit different vibrational properties as a result of a more open surface structure of the Al(001) substrate. Indeed, in this paper we show that for the ordered $c(2 \times 2)$ phases formed by the alkali atoms (Na and Li) on the Al(001) surface a distinct character of the adsorbate–substrate bonding results in a different behaviour of vibrational modes of alkalis.

The calculations are performed using the embedded-atom method (EAM) [24]. The EAM interatomic potentials used in the present work were applied before to the calculation of phonons on clean surfaces of Al, Na, Li and on the Al(111) surface covered by alkali adsorbates [10, 25–27]. The interaction between Al and AM atoms is described by a pair potential constructed in the form proposed in [28]. For phonon calculations we use a two-dimensional periodic slab consisting of 31 layers of Al (this thickness is sufficient to avoid interference effects) with $\frac{1}{2}$ ML of AM adsorbates on both sides. The atomic structures of the Al(001)-$c(2 \times 2)$-AM system with adatoms in different adsorption sites and the two-dimensional Brillouin zones (BZs) for the (1×1) and (2×2) unit cells are shown in figure 1.

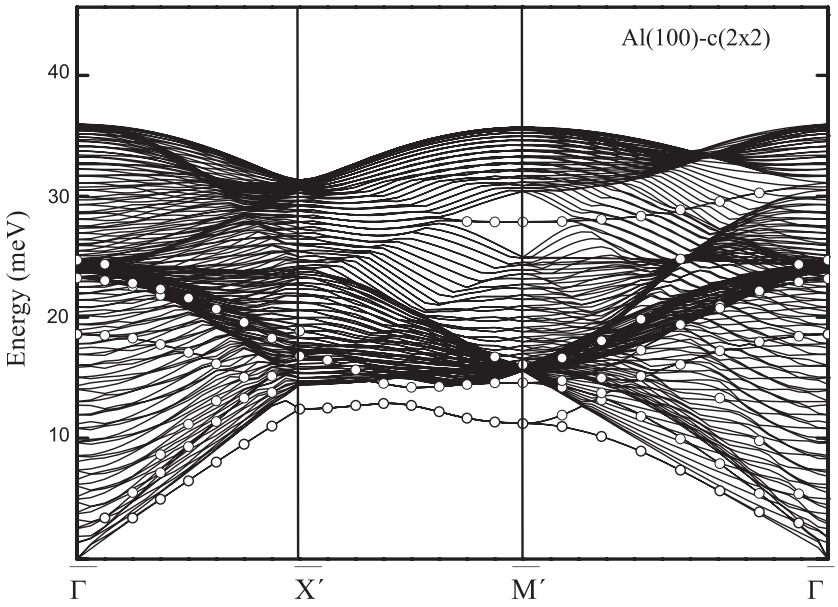

Figure 2. Calculated phonon dispersion curves for the Al(001) surface with $c(2 \times 2)$ unit cell. Surface states are shown by open circles.

2. Results and discussion

2.1. Clean Al(001) surface

Figure 2 shows the calculated phonon dispersion curves for the Al(001) surface with a $c(2 \times 2)$ unit cell so as to compare directly the vibrational properties of the clean and adsorbate-covered surfaces. In this case, the BZ is two times less than that for the (1×1) unit cell. This implies that the points of the original (1×1) BZ are folded into the points of the smaller (2×2) BZ as follows:

$$(2 \times 2) \begin{cases} \overline{\Gamma}, \overline{\mathrm{M}} \rightarrow \overline{\Gamma} \\ \overline{\mathrm{X}} \rightarrow \overline{\mathrm{M}'} \\ \frac{1}{2}\overline{\Gamma\mathrm{M}} \rightarrow \overline{\mathrm{X}'}, \end{cases}$$

where $\frac{1}{2}\overline{\Gamma\mathrm{M}}$ means a half of the segment $\overline{\Gamma\mathrm{M}}$. As a consequence, the number of phonon branches is two times that of the original (1×1) surface. For example, at the $\overline{\Gamma}$ point the phonon modes from the $\overline{\mathrm{M}}$ point of the unfolded BZ appear. Similarly, at the $\overline{\mathrm{M}}'$ point one can find the surface modes from the $\overline{\mathrm{X}}$ point of the (1×1) BZ. The calculated Rayleigh (RW) mode energy at the $\overline{\mathrm{X}}$ ($\overline{\mathrm{M}}'$) point (see table 1) agrees well with the value of 14.9 meV from the first-principles calculation [29] and is slightly smaller than the energy of 15.14 ± 0.62 meV obtained experimentally [30]. The calculated local density of states (LDOS) for the outermost three surface layers as well as for the central layer is shown in figure 3. Further, we will discuss the alterations of the surface phonon modes that are inherent to the clean Al(001) surface upon the alkali adsorption.

2.2. Al(001)-c(2 × 2)–Na

The atomic positions of the adsorbate and substrate atoms were relaxed to optimize the interlayer distances. For hollow adsorption sites the calculated nearest-neighbour Na–Al

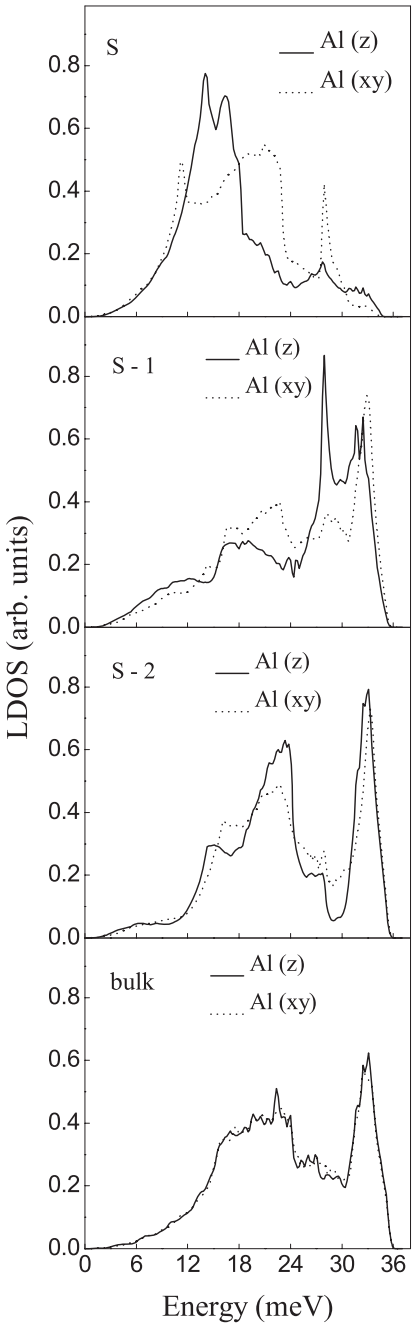

Figure 3. Local densities of phonon states for the clean Al(001) surface.

distance, $d_{\mathrm{Na-Al}}$, is found to be 3.24 Å. This value agrees well with both the experimental data, $d_{\mathrm{Na-Al}} = 3.20 \pm 0.03$ Å [17] and $d_{\mathrm{Na-Al}} = 3.27 \pm 0.01$ Å [19], and the *ab initio* total energy calculation, $d_{\mathrm{Na-Al}} = 3.13$ Å [14]. The obtained results also show a small contraction of the top interlayer spacing in the substrate, $\Delta_{12} = -1.67\%$ with respect to the bulk one. A similar value, $\Delta_{12} = -2.0\%$, was obtained in the *ab initio* total energy calculation [14]. The values

Table 1. Surface phonon energies (meV) and polarizations at the high-symmetry points of the BZ.

Surface	$\overline{\Gamma}$	polarization	$\overline{X'}$	polarization	$\overline{M}'$	polarization
Al(001)-$c(2\times2)$	18.32	Z_{Al_s}	12.41	Z_{Al_s}	11.17	$(XY)_{Al_s}$
	23.16	$(XY)_{Al_s}$	16.75	$(Y)_{Al_{s,s-1}}$	14.52	Z_{Al_s}
	24.65	$Z_{Al_{s-1}}$	18.78	$(XY)_{Al_s}$	16.01	$(XY)_{Al_{s-1}}$
					27.79	$(XY)_{Al_s}, Z_{Al_{s-1}}$
Al(001)-$c(2\times2)$–Na	9.88	$(XY)_{Na}$	7.98	Y_{Na}	9.93	$(XY)_{Al_s}$
(hollow)	10.75	$(XZ)_{Na}, Z_{Al_s}$	9.76	X_{Na}, Z_{Al_s}	10.42	$(XY)_{Na}, Z_{Al_s}$
	19.44	$(Z)_{Na}$	12.78	Z_{Na,Al_s}	14.60	$(XY)_{Al_s}$
	22.09	Z_{Al_s}	14.35	$X_{Na}, (XZ)_{Al_{s,s-1}}$	15.01	$Z_{Na}, (XY)_{Al_s}$
	24.40	Z_{Na,Al_s}	17.04	$Y_{Al_{s,s-1}}$	15.96	$(XY)_{Al_{s-1}}$
	24.57	Z_{Na}, Al_{s-1}	21.17	$X_{Na}, (XZ)_{Al_s}$	21.56	$X_{Na}, (XZ)_{Al_s}$
			24.56	$Z_{Na}, (X)_{Al_{s,s-1}}$	24.26	$Z_{Na}, (XZ)_{Al_{s-1}}$
					28.54	$(XY)_{Al_s}, Z_{Al_{s-1}}$
					30.11	$Z_{Na}, (XY)_{Al_s}$
Al(001)-$c(2\times2)$–Na	11.46	Z_{Na}	2.77	Z_{Na}, X_{Al_s}	5.50	$(XY)_{Na,Al_s}$
(substitutional)	11.80	Y_{Na}	10.38	X_{Na}, Z_{Al_s}	9.02	$(XY)_{Al_{s-1}}$
	21.10	Z_{Al_s}	13.77	$Z_{Na,Al_{s-2}}$	11.17	Z_{Na}
	22.33	$(XY)_{Na,Al_s}$	15.06	Y_{Na}	15.18	$Z_{Al_{s,s-2}}$
	22.91	$Z_{Al_{s-1}}$	16.01	$Y_{Al_{s,s-1}}$	19.11	$(XY)_{Al_{s-1}}$
			19.52	$X_{Na}, (XZ)_{Al_{s-1}}$	19.52	$Z_{Na}, (XZ)_{Al_{s-1}}$
			31.39	$Y_{Al_{s,s-1,s-2}}$	27.50	$X_{Na}, Y_{Al_s}, Z_{Al_{s-1}}$
			31.60	$Z_{Al_{s,s-2}}, X_{Al_{s-1}}$	29.12	$(XY)_{Al_{s-1}}$
					36.35	$Z_{Al_{s,s-2}}, X_{Al_{s-1}}$
Al(001)-$c(2\times2)$–Li	18.69	Z_{Al_s}	11.50	$Z_{Al_{s,s-1}}$	9.14	$(XY)_{Li,Al_s}$
(substitutional)	19.81	$(XY)_{Al_s}$	13.48	$X_{Al_s}, Z_{Al_{s-1}}$	11.90	$(XY)_{Al_{s-1}}$
	20.68	Z_{Li,Al_s}	16.87	$Y_{Al_{s,s-1}}$	13.57	Z_{Al_s}
	21.50	Z_{Li}	18.82	Z_{Li}, X_{Al_s}	16.58	$(XY)_{Al_{s-1}}$
	23.16	$Z_{Al_{s-1}}$	24.90	$Z_{Li}, (XZ)_{Al_{s-2}}$	23.04	$Z_{Li}, (XYZ)_{Al_{s-2}}$
	24.50	$Z_{Li}, (XZ)_{Al_{s-2}}$	27.75	$(XZ)_{Al_{s,s-1}}$	24.90	$Z_{Li,Al_{s-2}}$
	39.80	$(XY)_{Li}, Z_{Al_{s-1}}$	36.11	$(XY)_{Li}, Z_{Al_{s-1}}$	40.32	$(XY)_{Li,Al_s}, Z_{Al_{s-1}}$

reported in the LEED study [19] as well as in the *ab initio* pseudopotential calculation [21] reveal an expansion of 0.3% and 0.83%, respectively.

The calculated phonon dispersion for Al(001)-$c(2\times2)$–Na with adatoms in hollow sites is shown in figure 4(a). The surface mode energies at the high-symmetry points of the BZ are summarized in table 1. Figure 5(a) shows the local density of phonon states for the first three layers of the substrate and for adatoms. As one can see, the Na adsorption gives rise to two new surface modes below the bottom of the bulk spectrum. These frustrated translation (T) modes are associated with in-plane (XY-polarized) displacements of adsorbates. At the $\overline{X}'$ point their energies are 7.98 and 9.76 meV. These modes produce the main contribution to the in-plane adsorbate motion and appear in the corresponding LDOS as the most prominent feature, a double low-energy peak. The upper T mode, as can be seen from the local density of states, couples to the substrate acoustic shear-vertical (Z-polarized) modes. Similar adlayer T modes with a negligible dispersion but strong coverage dependence were also obtained for Na adsorbates on the Cu(001) and Cu(111) substrates [10, 31]. Another adsorbate-induced vibrational state was obtained at an energy of 19.44 meV at the $\overline{\Gamma}$ point. This resonance associated with adatom–substrate stretch (S) vibrations exists only at small wavevectors near

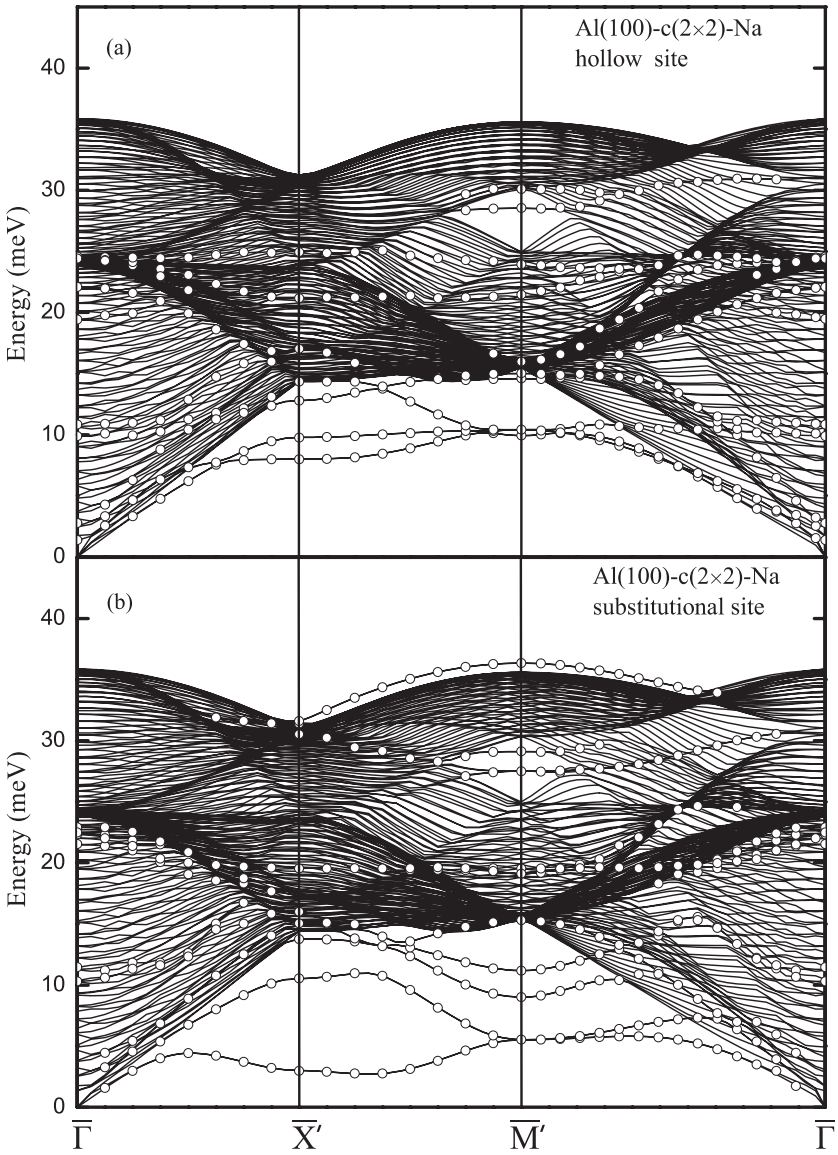

Figure 4. Calculated phonon dispersion curves for Al(001)-$c(2 \times 2)$–Na with sodium atoms in hollow (a) and substitutional (b) adsorption sites. Surface states are shown by open circles.

the BZ centre. The vibrational energy of the stretching mode was measured for Na adsorbates on the Cu(111) surface [32]. It was found to be ≈21 meV and almost independent of the coverage within the range 0–0.35 ML. In the *ab initio* calculations of one monolayer Na film on Cu(111) the same adatom–substrate stretch energy of 21 meV was derived from the curvature of the total energy with respect to displacements of a rigid adlayer relative to a rigid substrate [33]. Taking into account the substrate lattice dynamics influence, the value of 18 meV was obtained. At the monolayer saturation experimental data are also available for Na/Cu(001), where the S-mode vibrational energy is ≈18 meV [34]. A distinctive feature of the phonon spectrum is formed by two wide surface resonances which appear at energies of 21–25 meV. On the clean

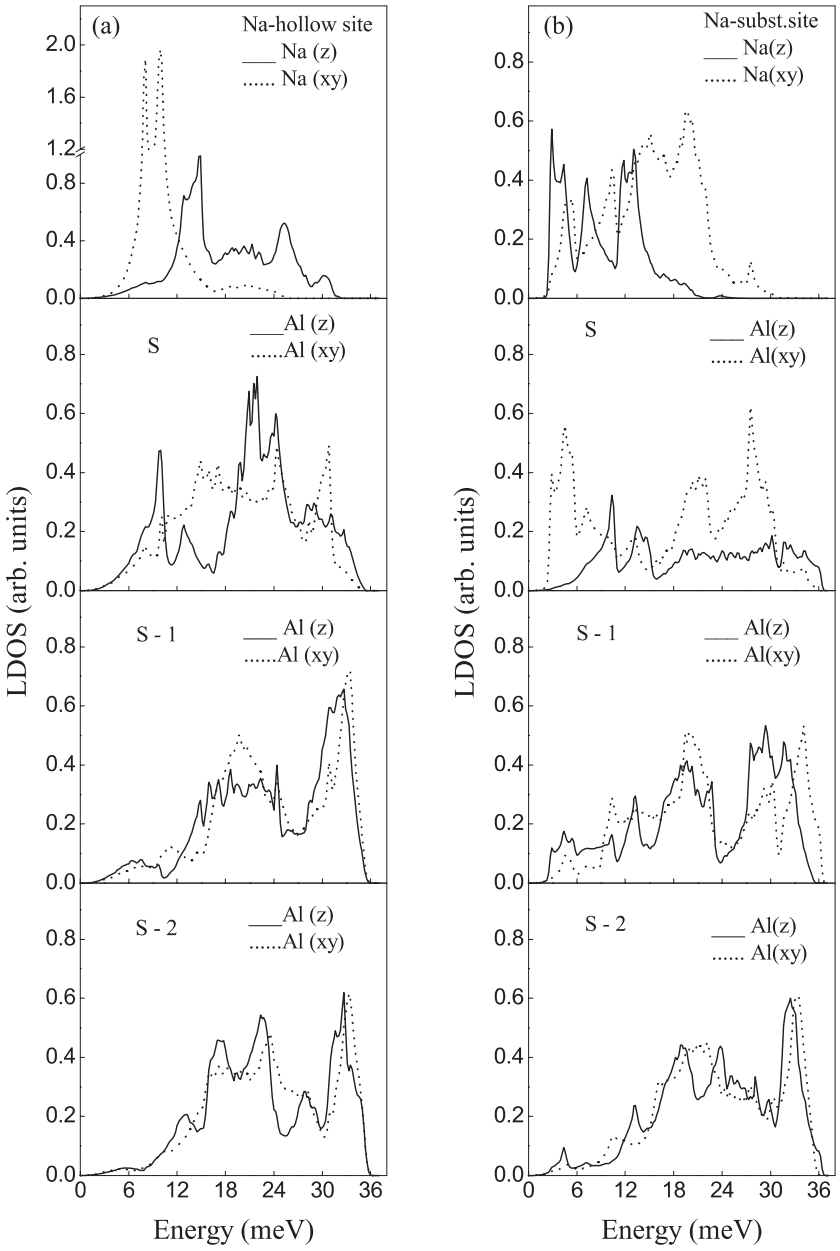

Figure 5. Local densities of states for Al(001)-$c(2 \times 2)$–Na with Na atoms in hollow (a) and substitutional (b) adsorption sites.

surface the upper mode mainly determined by the vertical motion of subsurface Al atoms exists only near the BZ centre. Upon Na adsorption, it couples to the adsorbate motion along the surface normal and spreads along the entire BZ, assuming a resonant character. An additional surface resonance, the lower one, is mainly determined by in-plane motion of Na adatoms. Their vibrational energies depend slightly on wavevectors, except that the lower one has a small dispersion on moving to the zone centre. A new adsorbate-induced surface resonance

also appears at the upper edge of the energy gap. As concerns the substrate atom vibrations, they change markedly, though most phonons which are localized at the clean surface remain, including the RW modes. The presence of adsorbates leads to an alteration of their frequencies and, as a rule, they now have a mixed character. Thus, the vibrational energies of shear-vertical modes become higher than those on the clean surface, as is evident from the LDOS for the top substrate layer (S). On the whole, upon Na adsorption the main peak in the vibrations normal to the surface is shifted towards higher energies and two additional peaks appear at lower energies. The lowest one corresponds to the substrate vibrations which couple to the in-plane motion of adsorbates and lie below the bulk continuum. The other, a smaller peak at 13–14 meV, is determined by the surface substrate modes which couple to the shear-vertical adsorbate motion. The latter, with an energy of 12.78 meV at the $\overline{\mathrm{X}}'$ point, splits off the bulk spectrum at the BZ boundary.

For substitutional adsorption sites the relaxation of the Al(001) substrate is found to be rather large. The relative contraction of the first interlayer spacing, Δ_{12}, is -8.8% with respect to the bulk value. This is in agreement with the value of $\Delta_{12} = -9.1 \pm 0.5\%$ obtained by LEED intensity analysis [19]. Another structural effect induced by Na adsorbates in substitutional sites is a small rippling which appears in the third Al layer, $\delta = 0.048$ Å. It means that Al atoms located directly beneath the Na adatoms move slightly towards the surface, while those located under the top layer Al atoms are repelled into the substrate (see figure 1(b)). The measured value of δ is 0.05 ± 0.02 Å [19]. The calculated bond length between the Na adatoms and the nearest-neighbour Al atoms, $d_{\mathrm{Na–Al}}$, is 3.09 Å. This value agrees well with both the experimental $d_{\mathrm{Na–Al}} = 3.07 \pm 0.01$ Å [19] and the *ab initio* calculated value of $d_{\mathrm{Na–Al}} = 3.02$ Å [14]. In this case the Na adatoms sit closer to the substrate than they do in hollow positions where the adsorbate–substrate height is twice as large (2.54 Å and 1.22 Å, respectively). This suggests a different adsorbate–substrate bonding. An indication of a similar deviation in the type of bonding for AM atoms in substitutional sites has been also reported for the Al(111)-($\sqrt{3} \times \sqrt{3}$)R30°–Na structure [13].

The phonon dispersion curves for Al(001)-$c(2 \times 2)$–Na with sodium in substitutional positions are shown in figure 4(b). In this case the mode associated with adatom–substrate stretch vibrations appears at lower energies, 11.46 meV at the $\overline{\Gamma}$ point. A similar resonance was observed for the Al(111)-($\sqrt{3} \times \sqrt{3}$)R30°–Na substitutional phase at 12.5 ± 0.2 meV [5] and was also obtained at an energy of 12.8 meV in the EAM calculations [10]. It is accompanied by another resonant mode which lies just above the first one and is mainly characterized by shear-horizontal displacements of adatoms. The vibrational amplitudes of both phonons decrease slowly on moving inside the substrate. As in the case of hollow site adsorption, two additional modes appear below the bulk phonon spectrum. But now both of them are characterized by displacements of adsorbates and the top-layer Al atoms in mutually perpendicular directions. The upper mode is mainly associated with in-plane displacements of adatoms and involves the vertical motion of the top substrate atoms. The lower one as well as the third mode from the bottom of the spectrum are mainly characterized by the adlayer motion normal to the surface. Unlike the case of hollow site adsorption, a new substrate surface mode is found above the bulk phonon spectrum. It is determined by the vertical motion of substrate atoms in the first and the third layers as well as by in-plane displacements of the subsurface Al atoms. Such a mode splitting above the bulk phonons is a typical feature for the case of a large surface relaxation and a substantial increasing of surface–subsurface interlayer interactions [35]. An analysis of the interatomic forces shows that the force constants between the topmost and subsurface substrate layers are increased by up to 20% as compared to those for the clean Al(001) surface. Another feature is that the interaction between the adsorbates and the nearest-neighbour substrate atoms is weaker than the Al–Al in-plane bonding in the top substrate layer.

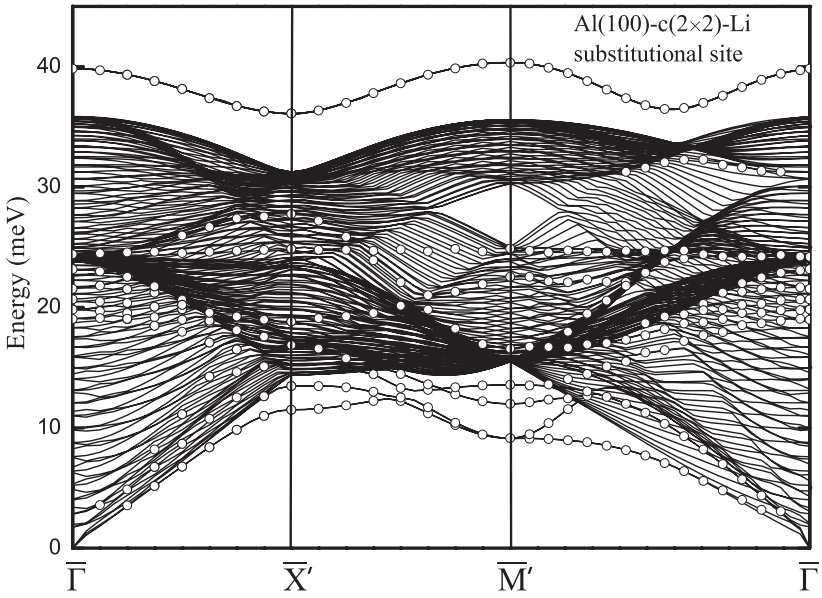

Figure 6. Calculated phonon dispersion curves for Al(001)-$c(2 \times 2)$–Li with lithium atoms in substitutional adsorption sites. Surface states are shown by open circles.

In contrast, for the Al(111)-($\sqrt{3} \times \sqrt{3}$)R30°–Na (Li) substitutional phases this interaction is rather strong [10]. The calculation also shows that the Na–Na interactions are not weak unlike the case of the Al(111) substrate where they are well screened by the surface electron density [14]. The calculated local density of states (figure 5(b)) shows that the shear-vertical displacements of adsorbates are now predominantly low-energy vibrations, while in the case of hollow site adsorption the low-energy adsorbate modes are associated, for the most part, with in-plane displacements in the adlayer. The next feature is connected with the shear-vertical motion of the top substrate atoms which is strongly suppressed as compared to the clean surface or to the case of hollow site adsorption.

2.3. Al(001)-c(2 × 2)–Li

As was shown by a quantitative LEED study [22, 23], the atomic structure of the Al(001)-$c(2 \times 2)$–Li phase formed by adsorption of $\frac{1}{2}$ ML Li on Al(001) at room temperature is a surface alloy with Li atoms in fourfold-coordinated substitutional sites. Like the previous cases of Na adsorption, the atomic positions of the adsorbate and substrate atoms were relaxed to obtain the equilibrium geometry. After relaxation, the distance between the Li adatoms and the nearest-neighbour substrate atoms, $d_{\mathrm{Li-Al}}$, is found to be 2.85 Å. This result agrees well with the value of $d_{\mathrm{Li-Al}} = 2.87$ Å obtained in the LEED study [23]. The calculated relative contraction of the topmost substrate interlayer spacing, Δ_{12}, is -3.8% with respect to the bulk distance. This value is smaller than $\Delta_{12} = -5.8 \pm 1.5\%$ obtained experimentally [22]. Like the previous case a small rippling appears in the third Al layer. The Al atoms lying just beneath the Li adatoms in the mixed Al/Li layer are displaced towards the surface by $\delta = 0.015$ Å.

The calculated phonon dispersion curves are shown in figure 6. As in the previous cases, at small wavevectors an adlayer localized resonance with vertical polarization of adatom displacements appears. At the $\overline{\Gamma}$ point its energy is 21.5 meV. This mode is accompanied by another adsorbate-induced resonance which is determined by shear-vertical displacements of

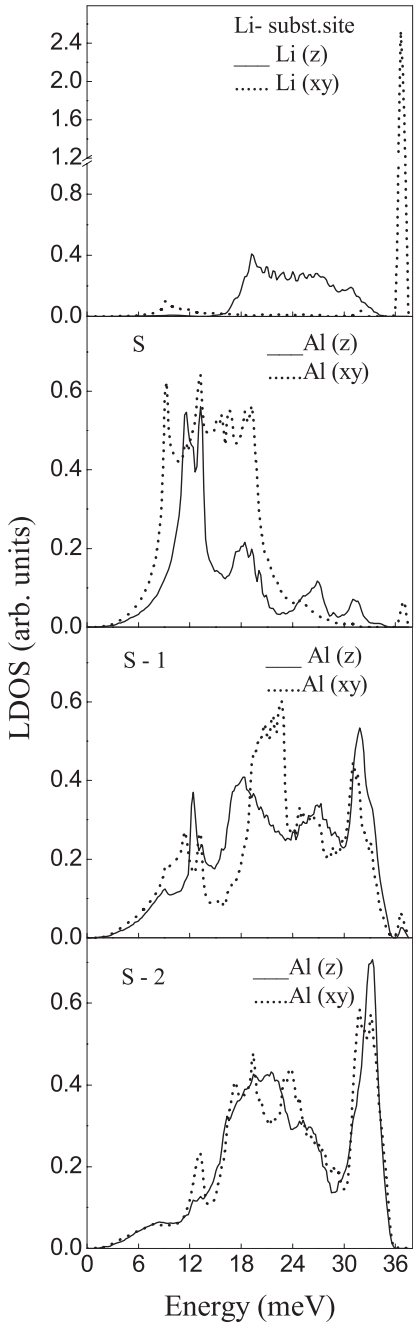

Figure 7. Local densities of states for the Al(001)-$c(2 \times 2)$–Li structure.

both adsorbates and substrate atoms and lies just below at 20.7 meV. A similar mode with a frequency of 21.3 meV at the $\overline{\Gamma}$ point was obtained for the Al(111)-($\sqrt{3} \times \sqrt{3}$)R30°–Li structure in the EAM calculations [10] and was observed in the high-resolution EELS (HREELS) measurements [5] at about 18 meV. Unlike the case of sodium, the surface modes

lying below the bulk phonons are localized on the substrate except for the lowest surface mode at the $\overline{\mathrm{M}}'$ point. The latter mainly associated with in-plane vibrations in the substrate involves partly the in-plane motion of Li (a small peak at ∼9 meV in the LDOS for Li, figure 7). On the whole, the modes associated with vibrations of Li adatoms shift towards the higher energies due to the reduced mass of the Li atoms, and most of them couple with the motion of substrate atoms. Thus, there is a pronounced peak in the LDOS for in-plane polarized adlayer modes above the bulk spectrum. It is determined by an optical mode strongly localized (90%) on the adlayer, though it also involves a small portion (10%) of in-plane displacements of the top substrate atoms and shear-vertical motion in the next substrate layer. This mode spreads over the entire BZ at energies around 36–40 meV. In the case of Na adsorption, such in-plane polarized adlayer modes were obtained below the bottom of the bulk phonon spectrum. Unlike the case of the Al(111) substrate, the density of phonon modes for vertically polarized vibrations of adatoms distributes over a wide energy range without any pronounced peak. The shear-vertical motion of the top substrate atoms does not change markedly as compared to the clean surface, as distinct from the case of Na substitutional adsorption, where it is substantially suppressed. Another feature is that the gap mode moves up towards the higher energies above the bulk phonon edge and becomes bulklike. The corresponding peak in the LDOS for in-plane motion of the top substrate atoms disappears.

3. Conclusion

We have presented the results of a theoretical study of the vibrational properties for the Al(001)-$c(2 \times 2)$–Na (Li) surface systems formed by adsorption of $\frac{1}{2}$ ML of AM at low and room temperatures. The calculated lengths of the AM–Al bonding are arranged in order of magnitude according to the adsorbate masses and are in agreement with the available experimental data. An analysis of the equilibrium structural characteristics shows that the effect of the AM adsorption on the Al substrate consists in a contraction of the outermost interlayer substrate spacing as compared to the clean surface. With Na (Li) adsorbates occupying substitutional sites this contraction becomes rather large. In this case the calculated interatomic forces show an increase by ∼20% of the force constants between the topmost and subsurface substrate atoms while the in-plane force constants remain nearly unchanged. Another structural effect induced by Na (Li) adsorbates in substitutional sites is a small rippling which appears in the third Al layer. The calculation shows that, upon the AM adsorption, most of the surface localized modes assume a mixed character coupling to the adsorbate motion. The interaction between adsorbates turned out not to be weak, unlike the case of the Al(111) substrate. For all the structures considered, a resonance associated with adatom–substrate stretch vibrations was obtained. The calculated stretching energies show that they depend on both the atomic masses and the adsorbate–substrate interaction.

Acknowledgments

The work was supported by the Federal Science and Innovation Agency of the Russian Federation, a grant from the Siberian Branch of the Russian Academy of Science (the integration project N 216) and the Basque Country Government.

References

[1] Bonzel H P, Bradshaw A M and Ertl G (ed) 1989 *Physics and Chemistry of Alkali Metal Adsorption* (Amsterdam: Elsevier)
[2] Diehl R D and McGrath R 1996 *Surf. Sci. Rep.* **23** 43

[3] Lindgren S-Å and Waldén L 1988 *Phys. Rev.* B **38** 3060
[4] Chulkov E V and Silkin V M 1989 *Surf. Sci.* **215** 385
[5] Nagao T, Iizuka Y, Shimazaki T and Oshima C 1997 *Phys. Rev.* B **55** 10064
[6] Witte G and Toennies J P 2000 *Phys. Rev.* B **62** R7771
[7] Chulkov E V, Kliewer J, Berndt R, Silkin V M, Hellsing B, Crampin S and Echenique P M 2003 *Phys. Rev.* B **68** 195422
[8] Borisova S D, Rusina G G, Eremeev S V, Benedek G, Echenique P M, Sklyadneva I Yu and Chulkov E V 2006 *Phys. Rev.* B **74** 165412
[9] Finberg S E, Lakin J V and Diehl R D 2002 *Surf. Sci.* **496** 10
[10] Rusina G G, Eremeev S V, Borisova S D, Sklyadneva I Yu and Chulkov E V 2005 *Phys. Rev.* B **71** 245401
[11] Andersen J 1995 *Surf. Rev. Lett.* **2** 345
[12] Adams D L 1996 *Appl. Phys.* A **62** 123
[13] Neugebauer J and Scheffler M 1992 *Phys. Rev.* B **46** 16067
[14] Stampfl C, Neugebauer J and Scheffler M 1993 *Surf. Sci.* **307–309** 8
[15] Nielsen M M, Christensen S V and Adams D L 1996 *Phys. Rev.* B **54** 17902
[16] Andersen J N, Lundgren E, Nyholm R and Qvarford M 1992 *Phys. Rev.* B **46** 12784
[17] Aminpirooz S, Schmalz A, Pangher N, Haase J, Nielsen M M, Batchelor D R, Bogh E and Adams D L 1992 *Phys. Rev.* B **46** 15594
[18] Fasel R, Aebi P, Osterwalder J, Schlapbach L, Agostino R G and Chiarello G 1994 *Phys. Rev.* B **50** 17540
[19] Berndt W, Weick D, Stampfl C, Bradshaw A M and Sheffler M 1995 *Surf. Sci.* **330** 182
[20] Stampfl C, Neugebauer J and Scheffler M 1994 *Surf. Rev. Lett.* **1** 213
[21] Oka K and Oguchi T 2001 *Surf. Sci.* **493** 99
[22] Petersen J H, Søndergard C, Hoffmann S V, Mikkelsen A and Adams D L 1999 *Surf. Sci.* **437** 317
[23] Petersen J H, Mikkelsen A, Nielsen M M and Adams D L 1999 *Phys. Rev.* B **60** 5963
[24] Foiles S M, Baskes M I and Daw M S 1986 *Phys. Rev.* B **33** 7983
[25] Chulkov E V and Sklyadneva I Yu 1995 *Surf. Sci.* **331–333** 1414
[26] Sklyadneva I Yu, Rusina G G and Chulkov E V 2002 *Phys. Rev.* B **65** 235419
[27] Sklyadneva I Yu, Chulkov E V and Bertsch A V 1996 *Surf. Sci.* **352–354** 25
[28] Johnson R A 1989 *Phys. Rev.* B **39** 12554
[29] Bohnen K P and Ho K M 1988 *Surf. Sci.* **207** 105
[30] Mohamed M H and Kesmodel L L 1988 *Phys. Rev.* B **37** 6519
[31] Graham A P, Toennies J P and Benedek G 2004 *Surf. Sci.* **556** L143
[32] Lindgren S-Å and Waldén L 1993 *J. Electron Spectrosc. Relat. Phenom.* **64/65** 483
[33] Carlsson J M and Hellsing B 2000 *Phys. Rev.* B **61** 13973
[34] Benedek G, Ellis J, Reichmuth A, Ruggerone P, Schief H and Toennies J P 1993 *Phys. Rev. Lett.* **69** 2951
[35] Dobrzynski L and Mills D L 1969 *J. Phys. Chem. Solids* **30** 1043